Journal of the
SOIL MECHANICS AND FOUNDATIONS DIVISION
Proceedings of the American Society of Civil Engineers

NONLINEAR ANALYSIS OF STRESS AND STRAIN IN SOILS

By James M. Duncan[1] and Chin-Yung Chang,[2]
Associate Members ASCE

INTRODUCTION

Before the development of electronic computers, it was not feasible to perform analyses of stresses in soil masses for other than assumed linear elastic soil behavior. Now, however, due to the availability of high-speed computers and powerful numerical analytical techniques such as the finite element method developed by Clough (4), it is possible to approximate nonlinear, inelastic soil behavior in stress analyses. In order to perform nonlinear stress analyses of soils, however, it is necessary to be able to describe the stress-strain behavior of the soil in quantitative terms, and to develop techniques for incorporating this behavior in the analyses.

A simplified, practical nonlinear stress-strain relationship for soils which is convenient for use with the finite element method of analysis is described herein, examples of its use are shown. Two of the parameters involved in this relationship are c and ϕ, the Mohr-Coulomb strength parameters. The other four parameters involved in the proposed relationship may be evaluated easily using the stress-strain curves of the same tests used to determine the values of c and ϕ.

STRESS-STRAIN CHARACTERISTICS OF SOILS

The stress-strain behavior of any type of soil depends on a number of different factors including density, water content, structure, drainage conditions, strain conditions (i.e. plane strain, triaxial), duration of loading, stress history, confining pressure, and shear stress. In many cases it may be possible

Note.—Discussion open until February 1, 1971. To extend the closing date one month, a written request must be filed with the Executive Director, ASCE. This paper is part of the copyrighted Journal of the Soil Mechanics and Foundations Division, Proceedings of the American Society of Civil Engineers, Vol. 96, No. SM5, September, 1970. Manuscript was submitted for review for possible publication on March 3, 1970.

[1] Assoc. Prof. of Civ. Engrg., Univ. of California, Berkeley, Calif.
[2] Soils Engr., Materials Research and Development Inc., Woodward-Clyde & Associates, Oakland, Calif.

to take account of these factors by selecting soil specimens and testing conditions which simulate the corresponding field conditions. When this can be done accurately, it would be expected that the strains resulting from given stress changes in the laboratory would be representative of the strains which would occur in the field under the same stress changes. Lambe (23,24) has described this procedure and explained how it may be used to predict strains and movements in soil masses, without developing a stress-strain relationship for the soil.

This same concept of duplicating field conditions can greatly simplify the procedures required for determining stress-strain relationships for soils; if soil specimens and test conditions are selected to duplicate the field conditions, many of the factors governing the stress-strain behavior of the soil will be accounted for. Even when this procedure is followed, however, it is commonly found that the soil behavior over a wide range of stresses is nonlinear, inelastic, and dependent upon the magnitude of the confining pressures employed in the tests. In the subsequent sections of this paper, a simplified, practical stress-strain relationship is described which takes into account the nonlinearity, stress-dependency, and inelasticity of soil behavior.

NONLINEARITY AND STRESS-DEPENDENCY

Nonlinearity.—Kondner and his coworkers (17,18,19,20) have shown that the nonlinear stress-strain curves of both clay and sand may be approximated by hyperbolae with a high degree of accuracy. The hyperbolic equation proposed by Kondner was

$$(\sigma_1 - \sigma_3) = \frac{\epsilon}{a + b\epsilon} \quad \ldots \quad (1)$$

in which σ_1 and σ_3 = the major and minor principal stresses; ϵ = the axial strain; and a and b = constants whose values may be determined experimentally. Both of these constants a and b have readily visualized physical meanings: As shown in Fig. 1, a is the reciprocal of the initial tangent modulus, E_I, and b is the reciprocal of the asymptotic value of stress difference which the stress-strain curve approaches at infinite strain $(\sigma_1 - \sigma_3)_{ult}$.

Kondner and his coworkers showed that the values of the coefficients a and b may be determined most readily if the stress-strain data are plotted on transformed axes, as shown in Fig. 2. When Eq. 1 is rewritten in the following form

$$\frac{\epsilon}{(\sigma_1 - \sigma_3)} = a + b\epsilon \quad \ldots \quad (2)$$

it may be noted that a and b = respectively, the intercept and the slope of the resulting straight line. By plotting stress-strain data in the form shown in Fig. 2, it is easy to determine the values of the parameters a and b corresponding to the best fit between a hyperbola (a straight line in Fig. 2) and the test data.

When this is done it is commonly found that the asymptotic value of $(\sigma_1 - \sigma_3)$ is larger than the compressive strength of the soil by a small amount. This would be expected, because the hyperbola remains below the asymptote at all finite values of strain. The asymptotic value may be related to the com-

pressive strength, however, by means of a factor R_f as shown by

$$(\sigma_1 - \sigma_3)_f = R_f (\sigma_1 - \sigma_3)_{ult} \quad \ldots\ldots (3)$$

in which $(\sigma_1 - \sigma_3)_f$ = the compressive strength, or stress difference at failure; $(\sigma_1 - \sigma_3)_{ult}$ = the asymptotic value of stress difference; and R_f = the failure ratio, which always has a value less than unity. For a number of different soils, the value of R_f has been found to be between 0.75 and 1.00, and to be essentially independent of confining pressure.

By expressing the parameters a and b in terms of the initial tangent modulus value and the compressive strength, Eq. 1 may be rewritten as

$$(\sigma_1 - \sigma_3) = \frac{\epsilon}{\left[\frac{1}{E_i} + \frac{\epsilon R_f}{(\sigma_1 - \sigma_3)_f}\right]} \quad \ldots\ldots (4)$$

This hyperbolic representation of stress-strain curves developed by Kondner

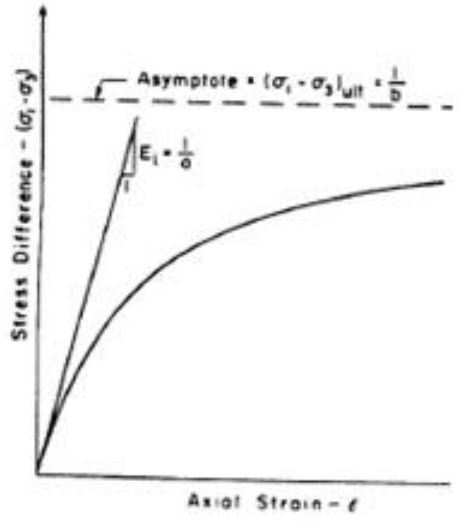

FIG. 1.—HYPERBOLIC STRESS-STRAIN CURVE

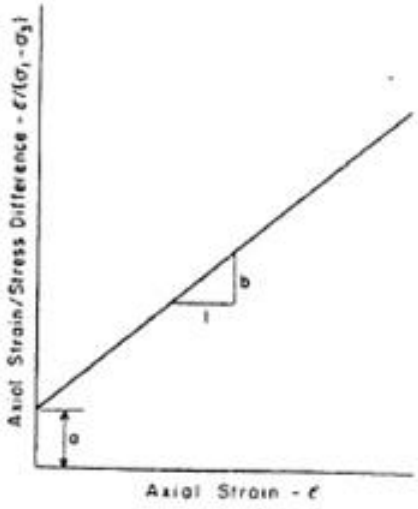

FIG. 2.—TRANSFORMED HYPERBOLIC STRESS-STRAIN CURVE

et al., has been found to be a convenient and useful means of representing the nonlinearity of soil stress-strain behavior, and forms an important part of the stress-strain relationship described herein.

Stress-Dependency.—Except in the case of unconsolidated-undrained tests on saturated soils, both the tangent modulus value and the compressive strength of soils have been found to vary with the confining pressure employed in the tests. Experimental studies by Janbu (14) have shown that the relationship between initial tangent modulus and confining pressure may be expressed as

$$E_i = K p_a \left(\frac{\sigma_3}{p_a}\right)^n \quad \ldots\ldots (5)$$

in which E_i = the initial tangent modulus; σ_3 = the minor principal stress; p_a = atmospheric pressure expressed in the same pressure units as E_i and

σ_3; K = a modulus number; and n = the exponent determining the rate of variation of E_i with σ_3; both K and n are pure numbers. Values of the parameters K and n may be determined readily from the results of a series of tests by plotting the values of E_i against σ_3 on log-log scales and fitting a straight line to the data, as shown in Fig. 3. The values shown in Fig. 3 were determined from the results of drained triaxial tests on a rockfill material used for the shell of Furnas Dam, and a silt from the foundation of Cannonsville Dam reported respectively by Casagrande (1), and Hirschfeld and Poulos (12).

If it is assumed that failure will occur with no change in the value of σ_3, the relationship between compressive strength and confining pressure may be expressed conveniently in terms of the Mohr-Coulomb failure criterion as

$$(\sigma_1 - \sigma_3)_f = \frac{2c \cos \phi + 2\sigma_3 \sin \phi}{1 - \sin \phi} \quad \ldots\ldots\ldots\ldots\ldots\ldots (6)$$

in which c and ϕ = the Mohr-Coulomb strength parameters.

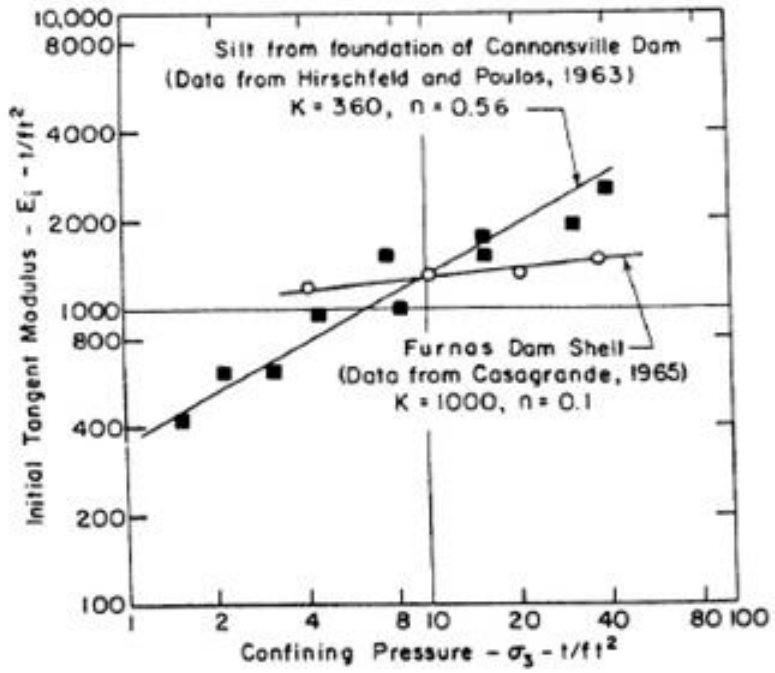

FIG. 3.—VARIATIONS OF INITIAL TANGENT MODULUS WITH CONFINING PRESSURE UNDER DRAINED TRIAXIAL TEST CONDITIONS

Eqs. 5 and 6, in combination with Eq. 4, provide a means of relating stress to strain and confining pressure by means of the five parameters K, n, c, ϕ, and R_f. Techniques for utilizing this relationship in nonlinear finite element stress analyses are analyzed in the following section.

PROCEDURES FOR NONLINEAR STRESS ANALYSES

Nonlinear, stress-dependent stress-strain behavior may be approximated in finite element analyses by assigning different modulus values to each of the elements into which the soil is subdivided for purposes of analysis, as shown

in Fig. 4. The modulus value assigned to each element is selected on the basis of the stresses or strains in each element. Because the modulus values depend on the stresses and the stresses in turn depend on the modulus values, it is necessary to make repeated analyses to insure that the modulus values and the stress conditions correspond for each element in the system.

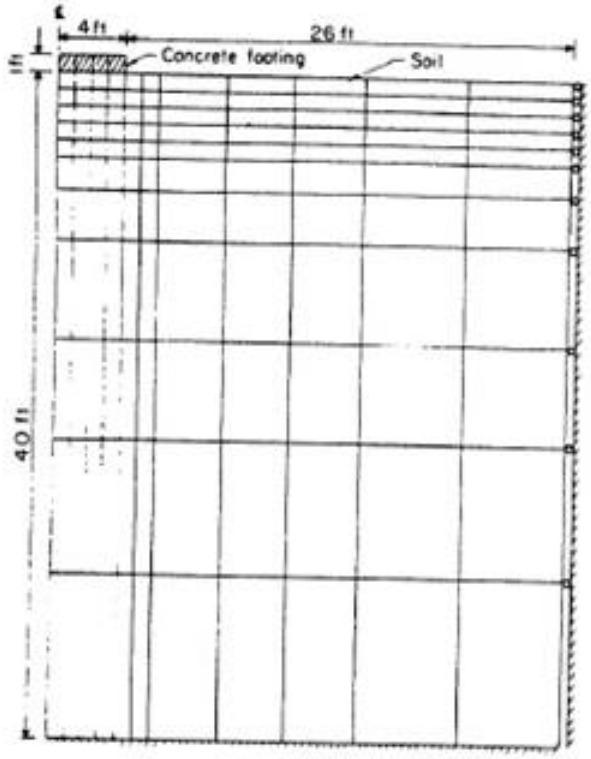

FIG. 4.—FINITE ELEMENT REPRESENTATION OF FOOTING ON SOIL

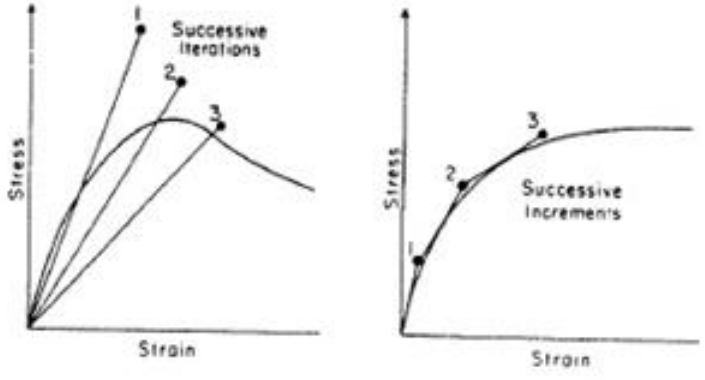

FIG. 5.—TECHNIQUES FOR APPROXIMATING NONLINEAR STRESS-STRAIN BEHAVIOR

Two techniques for approximate nonlinear stress analyses are shown in Fig. 5. By the iterative procedure, shown on the left-hand side of Fig. 5, the same change in external loading is analyzed repeatedly. After each analysis the values of stress and strain within each element are examined to determine

if they satisfy the appropriate nonlinear relationship between stress and strain. If the values of stress and strain do not correspond, a new value of modulus is selected for that element for the next analysis. This procedure has been applied to analyses of the load-settlement behavior of a footing on sand by Girijavallabhan and Reese (11) and to analyses of pavements by Duncan, Monismith and Wilson (8).

By the incremental procedure, shown on the right-hand side of Fig. 5, the change in loading is analyzed in a series of steps, or increments. At the beginning of each new increment of loading an appropriate modulus value is selected for each element on the basis of the values of stress or strain in that element. Thus the nonlinear stress-strain relationship is approximated by a series of straight lines. This procedure has been applied to analyses of embankments by Clough and Woodward (5), to analyses of excavated slopes by Dunlop and Duncan (10), and to analyses of stresses in simple shear specimens by Duncan and Dunlop (9).

Both of these methods have advantages and shortcomings. The principal advantage of the iterative procedure is the fact that it is possible, by means of this procedure, to represent stress-strain relationships in which the stress decreases with increasing strain after reaching a peak value. This capability may be very important because the occurrence of progressive failure of soils is believed to be associated with this type of stress-strain behavior. The shortcoming of the iterative procedure is that it is very difficult to take into account nonzero initial stresses, which plan an important role in many soil mechanics problems.

The principal advantage of the incremental procedure is that initial stresses may be readily accounted for. It also has the advantage that, in the process of analyzing the effects of a given loading, stresses and strains are calculated for smaller loads as well. For example, if the application of a 50-ton load to a footing was analyzed using 10 steps, or increments, the settlement of the footing, and the stresses and strains in the soil, would be calculated for footing loads in increments of 5 tons up to 50 tons. The shortcoming of the incremental procedure is that it is not possible to simulate a stress-strain relationship in which the stress decreases beyond the peak. To do so would require use of a negative value of modulus, and this cannot be done with the finite element method. The accuracy of the incremental procedure may be improved if each load increment is analyzed more than once. In this way it is possible to improve the degree to which the linear increments approximate the nonlinear soil behavior.

TANGENT MODULUS VALUES

The stress-strain relationship expressed by Eq. 4 may be employed very conveniently in incremental stress analyses because it is possible to determine the value of the tangent modulus corresponding to any point on the stress-strain curve. If the value of the minor principal stress is constant, the tangent modulus, E_t, may be expressed as

$$E_t = \frac{\partial(\sigma_1 - \sigma_3)}{\partial \epsilon} \qquad (7)$$

Performing the indicated differentiation on Eq. 4 leads to the following ex-

pression for the tangent modulus:

$$E_t = \frac{\frac{1}{E_i}}{\left[\frac{1}{E_i} + \frac{R_f \epsilon}{(\sigma_1 - \sigma_3)_f}\right]^2} \quad \ldots\ldots\ldots\ldots\ldots\ldots\ldots\ldots\ldots\ldots\ldots\ldots (8)$$

Although this expression for the tangent modulus value could be employed in incremental stress analyses, it has one significant shortcoming: The value of tangent modulus, E_t, is related to both stress difference and strain [$(\sigma_1 - \sigma_3)$ and ϵ], which may have different reference states. Although the reference state for stress difference [$(\sigma_1 - \sigma_3) = 0$] can be specified exactly, the reference state for strain ($\epsilon = 0$) is completely arbitrary. Thus, for example, the initial condition of a soil mass, before some external loading is applied, may rationally be referred to as the undeformed state, or state of zero strain. The same condition, however, could not be referred to as the state of zero stress difference if the mass contained nonhydrostatic stresses as a result of body forces or any other influence. For the purpose of analyzing the effects of newly applied external loads, therefore, the initial condition could be chosen as the reference state for strain but not for stress difference. Although the conditions of zero stress difference and zero strain coincide in the tests described previously, they do not in many important soil mechanics problems. Therefore, the expression for tangent modulus may be made more generally useful if it is made independent of stress or independent of strain. Because the reference state for strain is chosen arbitrarily, and because stresses may be calculated more accurately than strains in many soil mechanics problems, it seems logical to eliminate strain and express the tangent modulus value in terms of stress only.

The strain, ϵ, may be eliminated from Eq. 8 by rewriting Eq. 4 as

$$\epsilon = \frac{\sigma_1 - \sigma_3}{E_i \left[1 - \frac{R_f(\sigma_1 - \sigma_3)}{(\sigma_1 - \sigma_3)_f}\right]} \quad \ldots\ldots\ldots\ldots\ldots\ldots\ldots\ldots\ldots\ldots\ldots\ldots (9)$$

and substituting this expression for strain into Eq. 8. After simplifying the resulting expression, E_t may be expressed as

$$E_t = (1 - R_f S)^2 E_i \quad \ldots\ldots\ldots\ldots\ldots\ldots\ldots\ldots\ldots\ldots\ldots\ldots (10)$$

in which S = the stress level, or fraction of strength mobilized, given by

$$S = \frac{(\sigma_1 - \sigma_3)}{(\sigma_1 - \sigma_3)_f} \quad \ldots\ldots\ldots\ldots\ldots\ldots\ldots\ldots\ldots\ldots\ldots\ldots (11)$$

If the expressions for E_i, $(\sigma_1 - \sigma_3)_f$, and S given by Eqs. 5, 6 and 11 are substituted into Eq. 10, the tangent modulus value for any stress condition may be expressed as

$$E_t = \left[1 - \frac{R_f(1 - \sin\phi)(\sigma_1 - \sigma_3)}{2c\cos\phi + 2\sigma_3 \sin\phi}\right]^2 K p_a \left(\frac{\sigma_3}{p_a}\right)^n \quad \ldots\ldots\ldots\ldots (12)$$

This expression for tangent modulus may be employed very conveniently in incremental stress analyses, and constitutes the essential portion of the stress-strain relationship described herein. It may be employed in either ef-

fective stress analyses or total stress analyses. For effective stress analyses drained test conditions, with σ_3' constant throughout, are used to determine the values of the required parameters. For total stress analyses unconsolidated-undrained tests, with σ_3 constant throughout, are used to determine the parameter values.

It should be pointed out that the stress-strain relationship described has been derived on the basis of data obtained from standard triaxial tests in which the intermediate principal stress is equal to the minor principal stress, because in most practical cases only triaxial test data are available. However, this same relationship may be used for plane strain problems in which the intermediate principal stress is not equal to the minor principal stress, if appropriate plane strain test results are available. For cases in which three dimensional stresses and strains are involved, it may be desirable to include in a failure criterion or a stress-strain relationship of soils the effects of the value of the intermediate principal stress. However, until the results of tests employing more general loading conditions are available on a routine basis, it seems desirable to employ simplified stress-strain relationship such as the one described, which will provide sufficient accuracy for many practical purposes.

The usefulness of Eq. 12 lies in its simplicity with regard to two factors.

1. Because the tangent modulus is expressed in terms of stresses only, it may be employed for analyses of problems involving any arbitrary initial stress conditions without any additional complications.
2. The parameters involved in this relationship may be determined readily from the results of laboratory tests. The amount of effort required to determine the values of the parameters K, n, and R_f is not much greater than that required to determine the values of c and ϕ.

EXPERIMENTAL DETERMINATION OF PARAMETERS

To develop techniques for evaluating the parameters K, n, R_f, c, and ϕ, and to evaluate the usefulness of Eq. 12 for representing nonlinear, stress-dependent soil behavior, a number of tests have been conducted on a uniform fine silica sand. The first of these tests were standard drained triaxial compression tests, which were used to evaluate the parameters representing the behavior of the sand upon primary loading. Tests were also conducted to examine the stress-strain behavior of the sand during unloading and reloading.

The sand used in these studies is a uniform fine silica sand with subangular to subrounded particles. The sand was washed between the No. 40 and No. 100 sieves to obtain a uniform material which would not segregate during sample preparation. Tests were performed on specimens prepared at two different initial void ratios; Dense, $e = 0.50$, $D_r = 100\%$, which was the lowest void ratio obtainable by vibration in the saturated state; and Loose, $e = 0.67$, $D_r = 38\%$, which was the loosest condition which could be conveniently prepared on a routine basis. The specimens tested were initially 1.4 in. diam and 3.4 in. high, and were prepared using the techniques described by Lee and Seed (25). The specimens were tested using normal (unlubricated) caps and bases.

Primary Loading.—Two series of compression tests were conducted, on

dense and loose specimens, at effective confining pressures of 1 kg per sq cm, 3 kg per sq cm, and 5 kg per sq cm. The variations of stress difference and volume change with axial strain in these tests are shown in Figs. 6 and 7. It may be noted that the dense specimens dilated considerably during the tests, whereas the loose specimens compressed or dilated very little. The axial strains at failure were 2 % to 4 % for the dense specimens and 12 % to 16 % for the loose specimens. The strength parameters determined from these tests were $c_d = 0$, $\phi_d = 36.5°$ for the dense specimens, and $c_d = 0$, $\phi_d = 30.4°$ for the loose specimens.

The stress-strain data for the dense specimen tested at 5 kg per sq cm have been replotted on transformed axes in Fig. 8 for the purpose of deter-

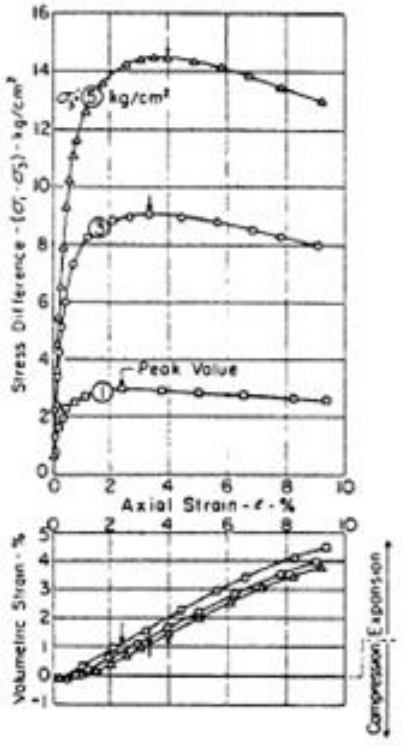

FIG. 6.—DRAINED TRIAXIAL TESTS ON DENSE SILICA SAND

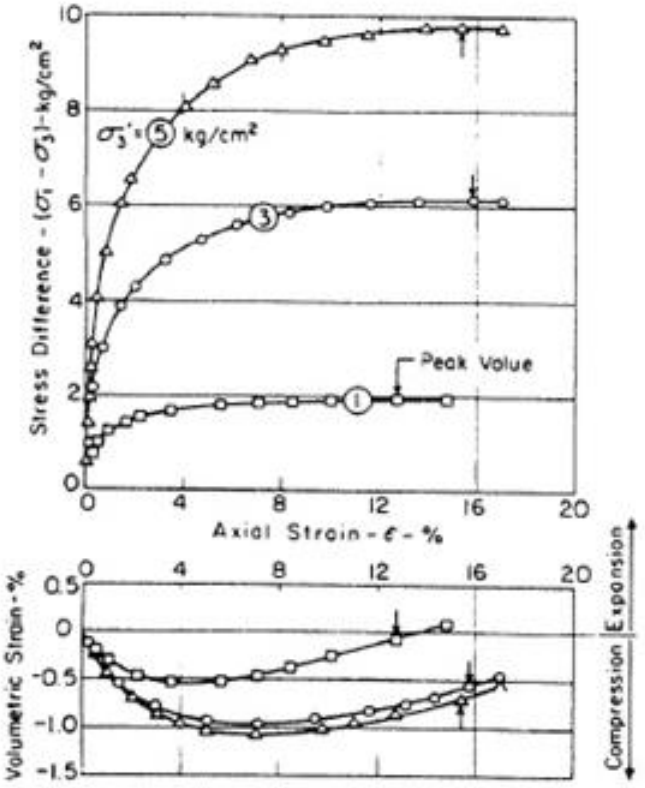

FIG. 7.—DRAINED TRIAXIAL TESTS ON LOOSE SILICA SAND

mining the values of E_i and $(\sigma_1 - \sigma_3)_{ult}$. It may be noted that data diverge somewhat from a linear relationship at both low and high values of strain, indicating that the stress-strain curve for this test is not precisely hyperbolic in shape. Nonetheless, a hyperbola may be fitted to these data at the origin $[(\sigma_1 - \sigma_3) = 0, \epsilon = 0]$ and at two other points. To reduce the degree of subjectivity involved in this procedure, it was found to be desirable to be consistent with regard to the values of stress level, S, at which the hyperbolae intersect the stress-strain curve. By repeated trials it was found that the best choices with regard to overall agreement were $S = 0.70$ and $S = 0.95$, or 70 % and 95 % strength mobilized. This same procedure has been found to work well for a variety of other soils as well.

The stress-strain data for the loose specimen tested at 5 kg per sq cm has been plotted on transformed axes in Fig. 9. It may be noted that these data diverge from a linear relationship also, but in the opposite way from the dense sand. The relationships shown in Figs. 8 and 9 have been found to hold in general; the transformed stress-strain data for dense specimens generally lie above the best-fit straight line at small values of strain, while the data for loose specimens generally lie below the best-fit straight line. Nevertheless, it has been found in every case to be possible to approximate the actual stress-strain curves by hyperbolae to a reasonable degree of accuracy.

The values of $(\sigma_1 - \sigma_3)_{ult}$ shown in Figs. 8 and 9 are somewhat larger than the values of stress difference at failure in these same tests, as was

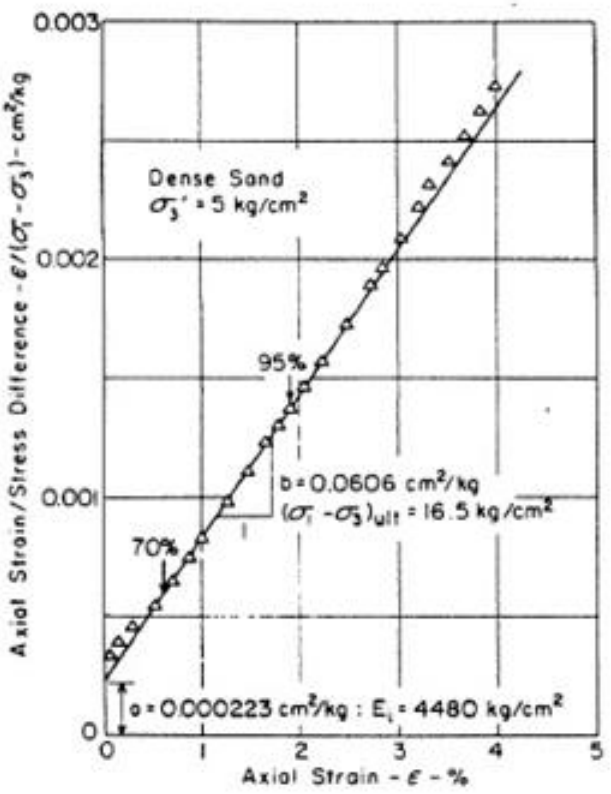

FIG. 8.—TRANSFORMED STRESS-STRAIN CURVE FOR DENSE SILICA SAND

mentioned previously. The values of R_f, which are a measure of this difference, were found to be 0.91 ± 0.03 for the dense sand, and 0.90 ± 0.05 for the loose sand. The values of E_i determined for all six tests have been plotted against the corresponding values of σ_3 in Fig. 10, for the purpose of determining the values of K and n. Linear interpretations of these data are shown in Fig. 10; the straight lines shown correspond to K = 2,000, n = 0.54 for the dense sand, and K = 295, n = 0.65 for the loose sand.

Unloading-Reloading.—Davis and Poulos (6), Makhlouf and Stewart (26), Karst, et al. (15), Ko and Scott (16), and Holubec (13) have shown that soil is an elasto-plastic material in the sense that strains induced upon primary loading are only partially recoverable upon unloading, and when reloaded it behaves nearly elastically. To study this aspect of the behavior of the silica

sand described previously, additional tests were conducted in which specimens were subjected to one or more cycles of unloading and reloading. The results of one of these tests on dense sand is shown in Fig. 11. It may be noted that for cycles of unloading and reloading the sand has a small amount of hysteresis, but is very nearly linear and elastic. Furthermore, the modulus values for both cycles of unloading-reloading are the same, even though they occur at different strains and stress levels. Tests conducted on loose specimens of this sand gave similar results, and similar behavior has been found to be characteristic of other soils by Ko and Scott (16). On the basis of these observations it seems reasonable to believe that the stress-strain behavior of soil on unloading and reloading may be approximated with a high

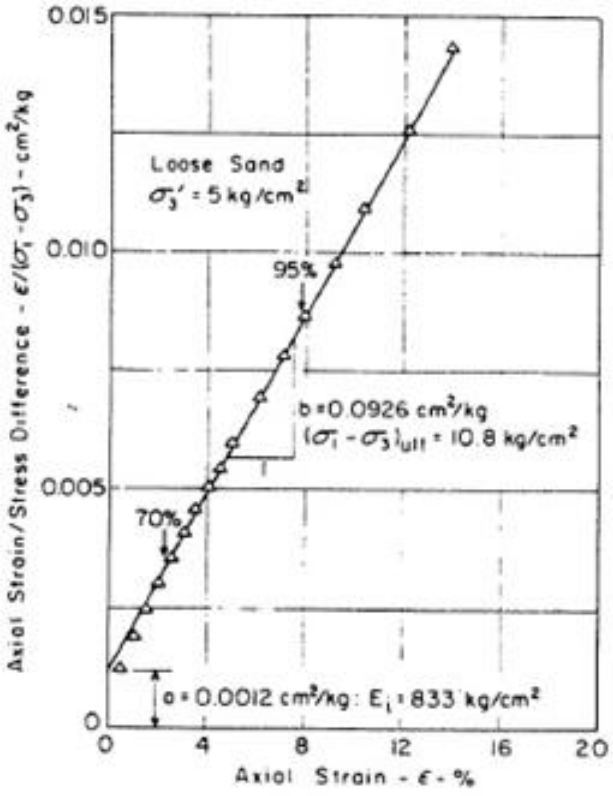

FIG. 9.—TRANSFORMED STRESS-STRAIN CURVE FOR LOOSE SILICA SAND

degree of accuracy as being linear and elastic. Because this linear behavior is independent of the value of stress difference, the representative modulus value is dependent only upon the confining pressure, σ_3.

The results of a number of tests involving unloading and reloading on the silica sand have shown that the variation of the modulus value with confining pressure may be represented by

$$E_{ur} = K_{ur} p_a \left(\frac{\sigma_3}{p_a}\right)^n \quad \ldots\ldots\ldots\ldots\ldots\ldots\ldots\ldots\ldots\ldots\ldots\ldots$$

in which E_{ur} = the unloading-reloading modulus value, and ... sponding modulus number. The influence of confining ... by the value of n, is for practical purposes the same ...

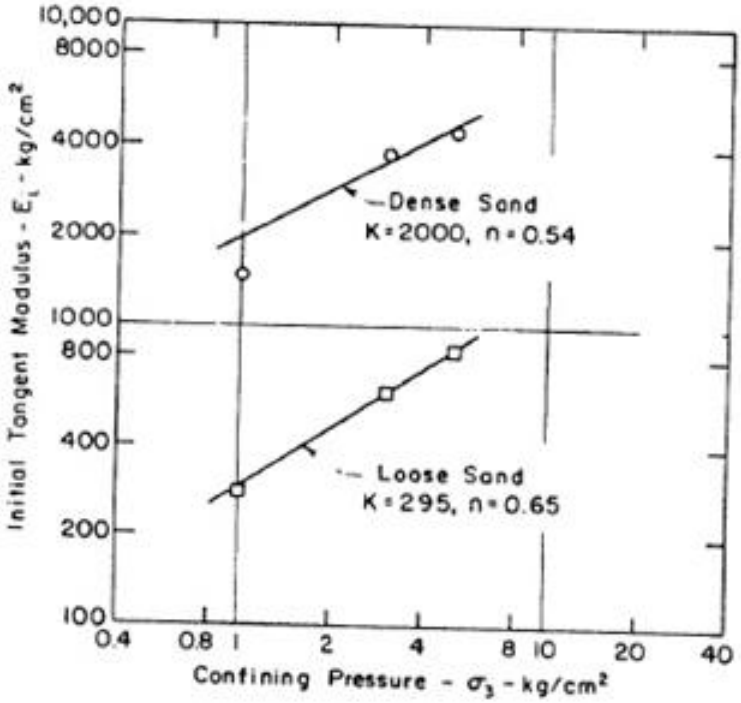

FIG. 10.—VARIATIONS OF INITIAL TANGENT MODULUS WITH CONFINING PRESSURE FOR DRAINED TRIAXIAL TESTS ON SILICA SAND

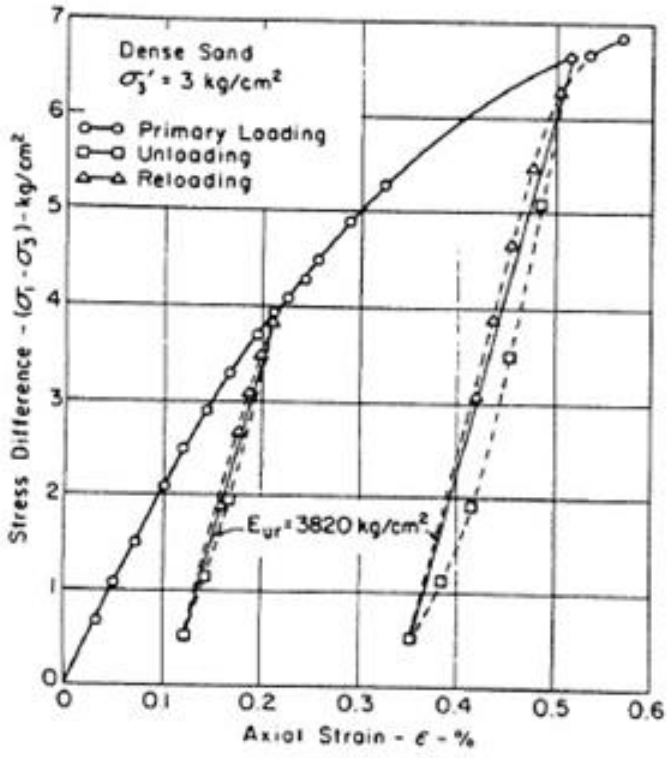

FIG. 11.—UNLOADING AND RELOADING OF SILICA SAND UNDER DRAINED TRIAXIAL TEST CONDITIONS

loading as for primary loading. The value of K_{ur} for unloading-reloading, however, is higher than for primary loading. For the silica sand in a dense condition K_{ur} was found to be 2,120, and for the loose condition 1,090.

Poisson's Ratio Values.—More than a single stress-strain coefficient is required to fully represent the mechanical behavior of any material under a general system of changing stresses. For isotropic materials, with no coupling between shear stresses and normal strains, two coefficients are required. For anisotropic materials, or materials which dilate or contract under the action of shear stresses, more than two coefficients are required. Many soils (including the silica sand tested in this study) exhibit clearly discernible dilatancy effects, and many soils are also anisotropic. Therefore it is likely that many stress-strain coefficients are required to characterize fully the complex stress-strain behavior of soils.

The main purpose of this investigation was to establish practical techniques for expressing the influence of stress level and confining pressure on

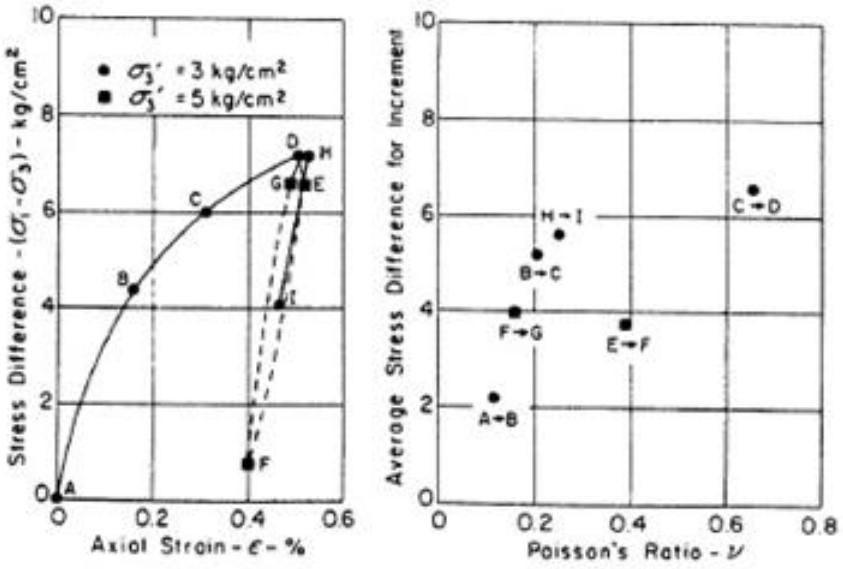

FIG. 12.—VALUES OF POISSON'S RATIO FOR DENSE SILICA SAND

tangent modulus values for soils, and other characteristics of soil stress-strain behavior have not been studied in detail. Instead, values of Poisson's ratio were calculated for increments of axial stress applied to the silica sand by means of

$$\nu = \frac{\Delta \epsilon_1 - \Delta \epsilon_v}{2\Delta \epsilon_1} \quad \ldots\ldots\ldots\ldots\ldots\ldots\ldots\ldots\ldots\ldots\ldots\ldots\ldots\ldots \quad (14)$$

in which ν = Poisson's ratio; ϵ_v and ϵ_1 = the volumetric and axial strains (compression positive); and Δ = an incremental change. Values of Poisson's ratio calculated from this expression are shown in Fig. 12 for a test on dense silica sand; the stress-strain increments to which the values apply are shown on the left-hand side. The values shown in Fig. 12 range from 0.11 to 0.65, generally increasing with increasing stress level on primary loading, as would be expected for a dense sand which dilates under large shear stresses. The values shown for unloading and reloading range from 0.15 to 0.4, and are

larger for unloading than for reloading. Values of Poisson's ratio calculated from the results of tests on loose sand were found to vary somewhat less with stress level, ranging from 0.26 to 0.41.

This study shows that it is not possible to characterize the behavior of the sand accurately by a single value of Poisson's ratio. Moreover, because the sand dilates under the action of shear stresses, the most appropriate stress-strain relationship would reflect the influence of shear stresses on volume changes. For the purposes of the studies described herein, however, it has been assumed that the soil may be characterized by a single constant value of Poisson's ratio, and no effort has been made to relate volume changes to shear stresses. The values of Poisson's ratio used in subsequent calculations were selected to represent, in a general way, the values of confining pressure and stress levels involved in the stress conditions analyzed. Studies of more accurate means of representing the volume change characteristics of soils are currently under way at the University of California.

Summary of Parameters.—The stress-strain parameters derived from the results of tests on the dense and loose silica sand are summarized in Table 1. These parameters may be used to calculate values of tangent modulus for

TABLE 1.—SUMMARY OF STRESS-STRAIN PARAMETERS FOR UNIFORM FINE SILICA SAND

Relative density (1)	ϕ_d, in degrees[a] (2)	R_f (3)	K (4)	K_{ur} (5)	n (6)
100 % (dense)	36.5	0.91	2,000	2,120	0.54
38 % (loose)	30.4	0.90	295	1,090	0.65

[a] $C_d = 0$ for dense and loose sand.

this sand for any combination of principal stresses defining a state of stress which is allowable in terms of the values of the shear strength parameters. Eq. 12 is used to evaluate the tangent modulus for primary loading, and Eq. 13 is used for unloading or reloading.

USE OF PARAMETERS TO PREDICT NONLINEAR BEHAVIOR

The stress-strain relationship described previously may be used very conveniently for incremental analyses of nonlinear behavior. The loading to be analyzed is divided into a number of increments, and for purposes of analysis the soil is assumed to behave linearly under each increment of load. If the increment involves primary loading, the modulus value for that increment is calculated using Eq. 12, which relates the tangent modulus to the average values of σ_1 and σ_3 during the increment by means of the experimentally determined parameters. If the increment involves unloading or reloading, the modulus value for that increment is calculated using Eq. 13.

The incremental strains for each load increment are related to the incremental stress changes for that increment by the generalized Hooke's law:

$$\Delta\epsilon_x = \frac{1}{E_t}\left[\Delta\sigma_x - \nu\left(\Delta\sigma_y + \Delta\sigma_z\right)\right] \quad \ldots\ldots\ldots\ldots\ldots\ldots \quad (15a)$$

$$\Delta\epsilon_y = \frac{1}{E_t}\left[\Delta\sigma_y - \nu\left(\Delta\sigma_z + \Delta\sigma_x\right)\right] \quad \ldots\ldots\ldots\ldots\ldots\ldots \quad (15b)$$

$$\Delta\epsilon_z = \frac{1}{E_t}\left[\Delta\sigma_z - \nu\left(\Delta\sigma_x + \Delta\sigma_y\right)\right] \quad \ldots\ldots\ldots\ldots\ldots\ldots \quad (15c)$$

$$\Delta\gamma_{xy} = \frac{2(1+\nu)}{E_t}\,\Delta\tau_{xy} \quad \ldots\ldots\ldots\ldots\ldots\ldots\ldots\ldots \quad (15d)$$

$$\Delta\gamma_{yz} = \frac{2(1+\nu)}{E_t}\,\Delta\tau_{yz} \quad \ldots\ldots\ldots\ldots\ldots\ldots\ldots\ldots \quad (15e)$$

$$\Delta\gamma_{zx} = \frac{2(1+\nu)}{E_t}\,\Delta\tau_{zx} \quad \ldots\ldots\ldots\ldots\ldots\ldots\ldots\ldots \quad (15f)$$

in which x, y, and z = orthogonal coordinate axes; $\Delta\epsilon$ = an incremental normal strain; $\Delta\gamma$ = an incremental shear strain; $\Delta\sigma$ = an incremental normal stress; $\Delta\tau$ = an incremental shear stress; E_t = the tangent modulus evaluated for the average stress conditions during the increment; and ν = Poisson's ratio. The cumulative strains at any stage of loading are calculated by summing the incremental values for all previous load increments. Cumulative stresses are calculated by summing the previous increments and the initial stresses. These techniques may be used to calculate strains under conditions where the stresses are known, or to perform incremental stress analyses. Examples of both of these types of application are described in subsequent sections.

Strains in Triaxial Tests.—The accuracy with which the nonlinear, stress-dependent stress-strain behavior of the sand can be represented by the relationship described previously is shown by the results in Figs. 13 through 16, which show comparisons of calculated and experimentally determined stress-strain curves. In each of these comparisons the values of stress were known apriori, and it was therefore unnecessary to perform finite element analyses of the stress changes. Instead the strains were calculated using a simple computer program which divides stress changes into small increments and calculates the corresponding strains using Eq. 15. Both the calculated and experimental curves shown in Figs. 13 through 16 are based on the assumption that the stress conditions in the triaxial specimens are completely uniform.

Stress-strain curves for tests with constant confining pressure are shown in Figs. 13 and 14, together with experimentally determined stress-strain curves for the same densities and values of confining pressure.

The calculated stress-strain curves for dense sand, shown in Fig. 13, consists of two parts: The first part of each stress-strain curve is a hyperbola extending up to the point where the strength of the sand is completely mobilized. At larger values of strain, where the hyperbola would indicate values of stress difference larger than the compressive strength, each stress-strain curve is represented by a nearly horizontal straight line corresponding to a very small positive modulus value. The calculated stress-strain curves for loose sand, shown in Fig. 14. consist of only one part, a hyperbola. There is no break-point on these curves because, for values of strain up to 16 %, the values of stress difference indicated by the hyperbolae do not exceed the compressive strength of the sand.

These comparisons serve to show the accuracy with which the nonlinear, stress-dependent stress-strain behavior of the sand can be represented over this range of pressures by the proposed relationship and the values of the parameters listed in Table 1. The approximations involved arise from: (1) Representation of the actual primary loading stress-strain curves by stress-strain curves of hyperbolic shape; (2) representation of the actual variation of initial tangent modulus with confining pressure by the exponential Eq. 5; and (3) representation of the actual strength characteristics of the sand by means of the Mohr-Coulomb Eq. 6. It may be seen that as a result of these approximations there is some difference between the experimental and calculated

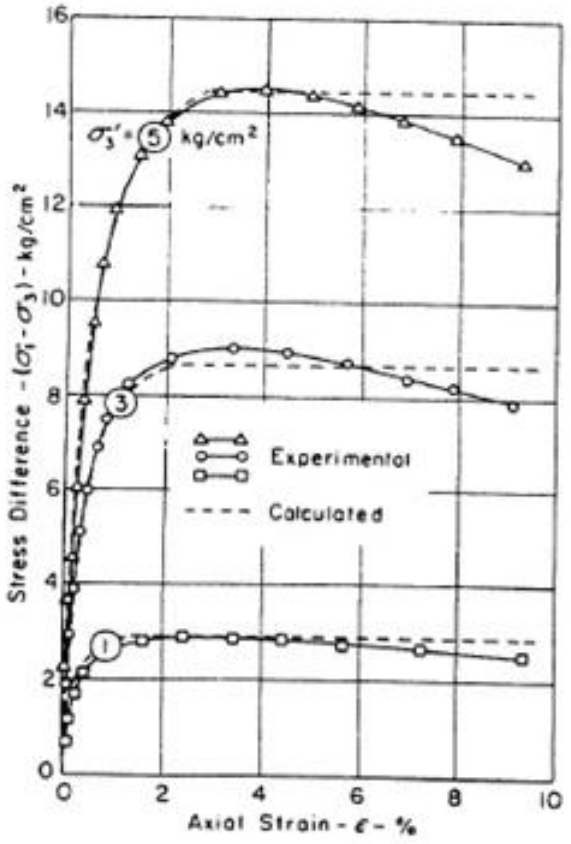

FIG. 13.—CALCULATED AND EXPERIMENTAL STRESS-STRAIN CURVES FOR DRAINED TRIAXIAL TESTS ON DENSE SILICA SAND

stress-strain curves in Figs. 13 and 14. The overall agreement, however, may be seen to be quite good, and it may be concluded that the primary loading behavior of the sand can be accurately represented by the proposed relationships.

The approximations involved in using the procedures described to calculate strains under conditions of changing confining pressure and unloading are shown by the calculated and experimental stress-strain curves compared in Figs. 15 and 16. In calculating the values of strain induced by changing confining pressure and unloading, it was assumed that the value of Poisson's ratio for the sand was 0.3, and values of unloading-reloading modulus were em-

ployed for any stage in a test for which the stress difference was smaller than the maximum value to which the specimen had previously been subjected.

The measured and predicted strains for one test on dense sand are shown on the right in Fig. 15. The changes in stress to which the specimen was subjected are shown on the left: The specimen was initially subjected to a hydrostatic pressure of 3 kg per sq cm (Point A). Then, at constant confining pressure, the stress difference was increased to 3.9 kg per sq cm (Point B), reduced to 0.5 kg per sq cm (Point C), increased to 6.65 kg per sq cm (Point D), reduced to 0.5 kg per sq cm (Point E), increased to 6.85 kg per sq cm (Point F), and reduced to 3.9 kg per sq cm (Point G). The confining pressure then was reduced to 2 kg per sq cm while the stress difference was increased to 4.15 kg per sq cm (Point H), and, finally, the stress difference was reduced to 0.6 kg per sq cm (Point I). The measured strains for these stress changes

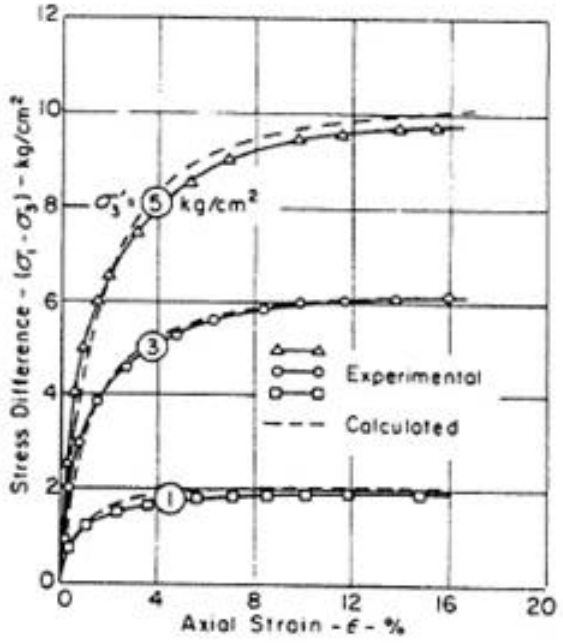

FIG. 14.—CALCULATED AND EXPERIMENTAL STRESS-STRAIN CURVES FOR DRAINED TRIAXIAL TESTS ON LOOSE SILICA SAND

are shown on the right in Fig. 15 by solids lines, and the calculated values are shown by dashed lines. The agreement between the calculated and experimental curves is very good; the curves have the same shape, and the maximum difference between the calculated and measured values of strain is about 0.7 % at Point F. Thus, although the values of the stress-strain parameters listed in Table 1 were derived from the results of standard tests conducted with constant values of σ_3, they provide a good evaluation of the strains in the soil under conditions of changing σ_3, if the average values of σ_3 are used for purposes of evaluating the tangent modulus, and the strains induced by all stress changes are accounted for as shown by Eq. 15.

The results of a similar test on loose sand is shown in Fig. 16. This specimen was subjected to the loading path ABCDEFG shown on the left. The predicted stress-strain behavior, shown by dotted lines, is in excellent agreement with that measured. The maximum difference between the calculated and ex-

perimentally determined values of strain is about 0.2 % midway between points A and B. It may be noted that the strains in this test on loose sand are about 10 times as large as those in the test on dense sand considered previously.

Example Nonlinear Finite Element Analyses.—To show the use of the procedures described for purposes of performing finite element stress analyses, computations have been made of the load-settlement relationships for a foot-

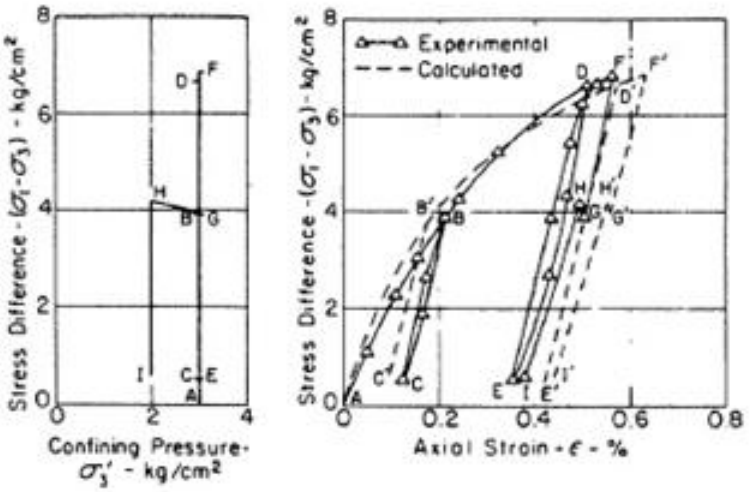

FIG. 15.—CALCULATED AND EXPERIMENTAL STRESS-STRAIN CURVES FOR DENSE SILICA SAND UNDER COMPLEX LOADING CONDITIONS

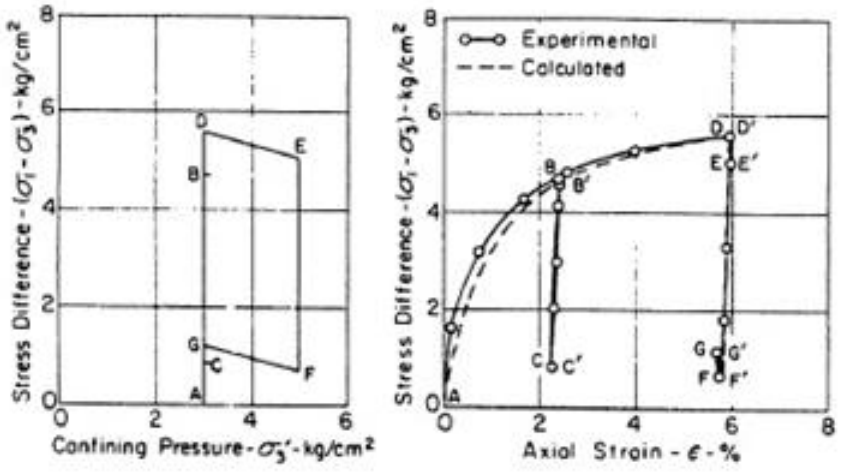

FIG. 16.—CALCULATED AND EXPERIMENTAL STRESS-STRAIN CURVES FOR LOOSE SILICA SAND UNDER COMPLEX LOADING CONDITIONS

ing in sand and for a footing on clay. Both analyses were performed using the same incremental analysis procedures: The modulus value of each element under each load increment was evaluated by means of Eq. 12, using estimated average values of stress for the increment; these values of stress were estimated by linear extrapolation of the previously calculated load-induced stresses. Using the sum of the estimated values of the load-induced stresses and the stresses due to gravity, values of σ_1 and σ_3 were calculated

which were used to evaluate the modulus for each element by means of Eq. 12.

Footing in Sand.—A finite element computer program employing the features described previously was used for analysis of the settlement of a model footing. The footing was 2.44 in. wide by 12.44 in. long and was installed at a depth of 20 in. in Chatahoochee River sand (7). The finite element mesh used in the analysis contained 204 elements and 234 nodal points as shown in Fig. 17. The footing was represented in the plane strain analysis by a strip footing of the same width. The model footing was constructed so that the base of the

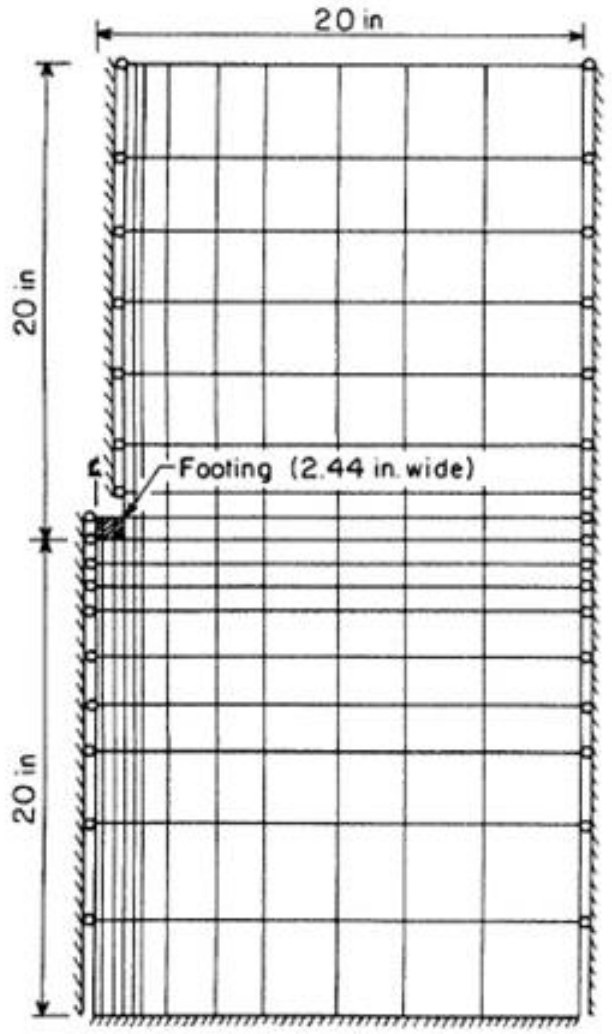

FIG. 17.—FINITE ELEMENT REPRESENTATION OF MODEL FOOTING IN SAND

footing could be loaded separately from the "skin" area of the shaft; accordingly, the footing was represented by a single row of elements with large modulus values, and the skin was represented as a frictionless vertical surface, as shown in Fig. 17. Loads were applied to the three elements representing the footing in increments of 2.5 psi. The nodal points along the centerline beneath the footing and those on the right vertical boundary were constrained to move only in the vertical direction, whereas those on the bottom boundary were constrained from either horizontal or vertical movement.

The rest of the nodal points, including those at the surface, were unconstrained. The three columns of elements above the footing, although actually represented in the analysis, were assigned very small modulus values to represent air, and are not shown in Fig. 17.

Although it would be desirable to employ values of K, n, ϕ, and R_f determined from the results of plane strain tests for this analysis, only triaxial test results were available. The values of K, n, ϕ and R_f shown in Fig. 18 were determined from the results of three triaxial tests at lower confining pressures on Chatahoochee River sand which were conducted by Vesić and Clough (27). The value of ν was estimated based on their results which showed that at high confining pressures the value of Poisson's ratio varied from about 0.25 to 0.30, increasing with increasing confining pressure. Because of the stronger tendency for the sand to dilate at lower confining pressures, it would be expected that the value of Poisson's ratio would be on the order of 0.35 at lower pressures, and this value was used in the finite element analysis.

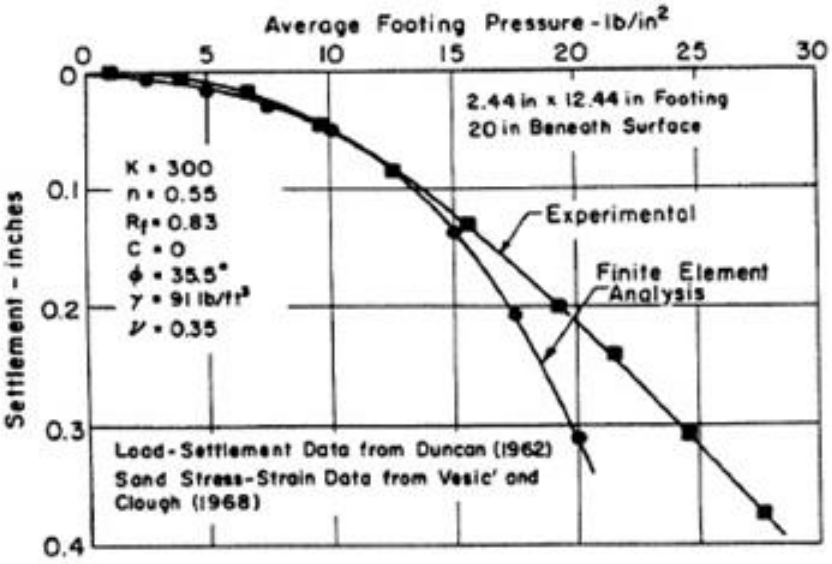

FIG. 18.—NONLINEAR FINITE ELEMENT ANALYSIS OF MODEL FOOTING IN SAND

Both the observed and calculated load-settlement curves are shown in Fig. 18. At large values of settlement the calculated load-settlement curve is steeper than the experimental curve. The shape of this portion of the calculated curve is affected by the value of ϕ employed in the analysis; it would be expected that if a larger value of ϕ determined from plane strain test results was used in the analysis, this part of the curve would be somewhat flatter. The shape of the final portion of the curve is also affected to some degree by the value of modulus assigned to elements after failure, which was arbitrarily taken to be 10 psf, and by the value of Poisson's ratio, which was estimated on the basis of results at higher pressures. For settlements smaller than about 10 % of the footing width, which could be considered to be the range of greatest practical interest, the calculated and experimental curves are in excellent agreement, the two values of pressure corresponding to the same settlement differing at most by about 15 %. It is interesting to note that the value of ultimate bearing capacity for this footing, calculated using the Ter-

zaghi bearing capacity factors, is 54 psi. This value of pressure corresponds to a very large settlement of the model footing, on the order of two-thirds of the width of the footing.

Footing on Clay.—The same finite element computer program, which may be employed for either plane strain or axisymmetric problems, was used to calculate the load-settlement curve for a hypothetical 8-ft diam circular footing on the surface of a layer of saturated clay. The axisymmetric finite element mesh employed in this analysis is the one shown in Fig. 4, which contains 125 elements and 149 nodal points. The mesh extends to a radial distance of 26 ft from the edge of the footing and to a depth of 40 ft below the footing. Nodal points on the radial boundary are constrained to move vertically only while those along the base were fixed. Loads were applied to the footing in increments of 0.25 tons per sq ft.

The calculated load-settlement curve for the footing is shown in Fig. 19 together with the values of the parameters employed in the analysis. The un-

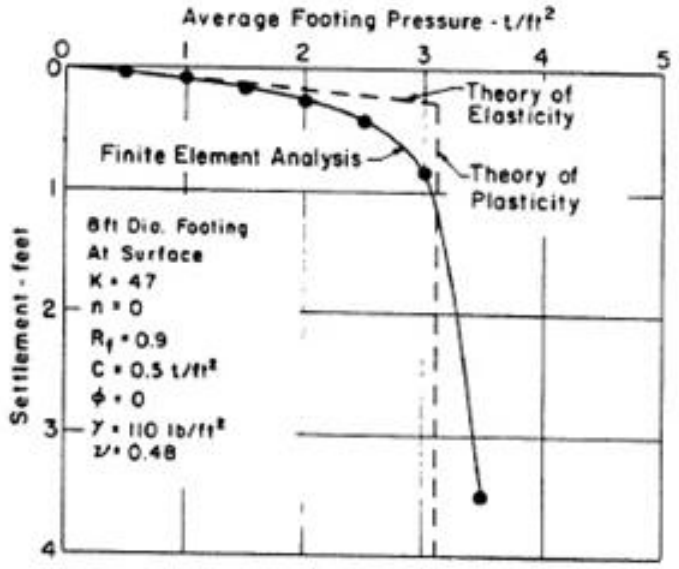

FIG. 19.—NONLINEAR FINITE ELEMENT ANALYSIS OF FOOTING ON CLAY

drained shear strength of the clay (0.5 tons per sq ft) and the initial tangent modulus value (50 tons per sq ft) were constant throughout the depth of the layer. It may be noted that the initial portion of the load-settlement curve is in good agreement with elastic settlements calculated using

$$\rho = \frac{qB}{E}\,(1 - \nu^2)\,I_\rho \qquad (16)$$

in which ρ = the vertical settlement; q = the average footing pressure; and I_ρ = a settlement influence factor which depends on the footing shape and the depth of the compressible layer. The elastic settlement shown in Fig. 19 was calculated using a settlement influence factor equal to 0.69 for a rigid circular footing on an incompressible elastic layer with a depth equal to five times the footing width, together with the initial tangent modulus value (50 tons per sq ft.)

The ultimate bearing capacity of the footing was calculated using

$$q_{ult} = cN_c \quad \ldots\ldots\ldots\ldots\ldots\ldots\ldots\ldots\ldots\ldots\ldots\ldots\ldots\ldots\ldots\ldots\ldots\ldots \quad (17)$$

in which c = the undrained shear strength and N_c = a bearing capacity factor derived from the theory of plasticity; a value of N_c equal to 6.2 was used to calculate the ultimate load for this circular footing at the surface. For settlements larger than about 1 ft, the finite element analysis load-settlement curve indicates bearing pressure values slightly larger than the ultimate bearing capacity calculated using Eq. 17. It may be noted, however, that the calculated settlements increase very rapidly at these large values of pressure indicating good agreement between the results of the finite element analysis and the theory of plasticity.

ANALYSIS AND CONCLUSION

The objective of this paper is to develop a simple, practical procedure for representing the nonlinear, stress-dependent, inelastic stress-strain behavior of soils. Accordingly, the relationship described has been developed in such a way that the values of the required parameters may be derived from the results of standard laboratory triaxial tests. If appropriate experimental results are available, the parameter values may instead be derived from the results of triaxial tests with lubricated caps and bases or from the results of plane strain compression tests.

With regard to its simplicity and the limitations attendant upon its use, the relationship described herein may be compared with the Mohr-Coulomb failure criterion. For example while it may be desirable from a theoretical standpoint to include in a failure criterion or a stress-strain relationship for soils the effects of the value of the intermediate principal stress, this is undesirable from a practical standpoint at the present time, because the required test results indicating these effects are seldom if ever available. Until the results of tests employing more general loading conditions are available on a routine basis, it seems desirable to employ stress-strain relationships based on the results of tests, like the standard triaxial test, which employ less general loading conditions but which are more frequently available. The use of simplified procedures and tests will result in some loss of accuracy, but the results will be sufficiently accurate for many practical purposes.

Although the stress-strain relationship described previously has some limitations owing to its simplicity, it incorporates three very important aspects of the stress-strain behavior of soils; nonlinearity, stress-dependency, and inelasticity, and it provides simple techniques for interpreting the results of laboratory tests in a form which may be used very conveniently in finite element stress analyses of soil masses. By means of this relationship the tangent modulus for soils may be expressed in terms of total stresses in the case of unconsolidated-undrained tests, or effective stresses in the case of drained tests. Similarly, the relationship may be used for stress analyses in terms of total or effective stresses, whichever is consistent with the tests performed and the conditions analyzed.

The relationship contains six parameters, whose values may be determined very readily from the results of a series of triaxial or plane strain compression tests involving primary loading, unloading, and reloading. Two of these parameters are the Mohr-Coulomb strength parameters, c and ϕ, and the other four also have easily visualized physical significance.

Comparisons of calculated and measured strains in specimens of dense and loose silica sand have shown that the relationship is capable of accurately representing the behavior of this sand under complex triaxial loading conditions, and analyses of the behavior of footings on sand and clay have shown that finite element stress analyses conducted using this relationship are in good agreement with empirical observations and applicable theories. These procedures have also been applied to a number of practical problems (Chang and Duncan, 2; Clough and Duncan, 3; Kulhawy and Duncan, 21, Kulhawy and Duncan, 22). In these cases it has been found that calculated soil movements were in good agreement with those determined by field instrumentation studies.

ACKNOWLEDGMENTS

The studies described were performed while the second writer held the Albert L. Ehrman Memorial Scholarship at the University of California. G. Pelatowsky did the drafting and N. Hoes typed the text.

APPENDIX I.—REFERENCES

1. Casagrande, A., "High Dams," Communications of the Institute for Foundation Engineering and Soil Mechanics, Technical Hochschule of Vienna, H. Borowicka, ed., No. 6, Vienna, Dec. 1965.
2. Chang, C-Y, and Duncan, J. M., "Analysis of Soil Movements Around Deep Excavation," *Journal of the Soil Mechanics and Foundations Division*, ASCE, Vol. 96, No. SM5, Proc. Paper , September, 1970, pp. .
3. Clough, G. W. and Duncan, J. M., "Finite Element Analyses of Port Allen and Old River Locks," *Report No. TE 69-3*, Office of Research Services, University of California, Berkeley, 1970.
4. Clough, R. W., "The Finite Element Method in Plane Stress Analysis," *Proceedings of the 2nd ASCE Conference on Electronic Computation*, Pittsburgh, 1960.
5. Clough, R. W., and Woodward, Richard J., III, "Analysis of Embankment Stresses and Deformations," *Journal of the Soil Mechanics and Foundations Division*, ASCE, Vol. 93, No. SM4, Proc. Paper 5329, July, 1967, pp. 529–549.
6. Davis, E. H., and Poulos, H. G., "Triaxial Testing and Three-Dimensional Settlement Analysis," *Proceedings*, of the 4th Australia-New Zealand Conference on Soil Mechanics and Foundation Engineering, 1963, p. 233.
7. Duncan, J. M., "The Influence of Depth on the Bearing Capacity of Strip Footings in Sand," thesis presented to the Georgia Institute of Technology, at Atlanta, Georgia, in 1962, in partial fulfillment of the requirements for the degree Master of Science.
8. Duncan, J. M., Monismith, C. L., and Wilson, E. L., "Finite Element Analyses of Pavements," *Proceedings of the 1968 Annual Meeting of the Highway Research Board*, 1968.
9. Duncan, J. M. and Dunlop, P., "Slopes in Stiff-Fissured Clays and Shales," *Journal of the Soil Mechanics and Foundations Division*, ASCE, Vol. 94, No. SM2, Proc. Paper 6449, March, 1969, pp. 467–492.
10. Dunlop, P., and Duncan, J. M., "Development of Failure Around Excavated Slopes," *Journal of the Soil Mechanics and Foundations Division*, ASCE, Vol. 95, No. SM2, Proc. Paper 7162, March, 1970, pp. 471–494.
11. Girijavallabhan, C. V., and Reese, L. C., "Finite Element Method for Problems in Soil

Mechanics," *Journal of the Soil Mechanics and Foundations Division*, ASCE, Vol. 94, No. SM2, Proc. Paper 5864, March, 1968, pp. 473–496.
12. Hirschfeld, R. C., and Poulos, S. J., "High Pressure Triaxial Tests on a Compacted Sand and on Undisturbed Silt," Laboratory Shear Testing of Soils, American Society for Testing and Materials, *Special Technical Publications, No. 361*, Ottawa, 1963.
13. Holubec, I., "Elastic Behavior of Cohesionless Soil," *Journal of the Soil Mechanics and Foundations Division*,ASCE, Vol. 94, No. SM6, Proc. Paper 6216, November, 1968, pp. 1215–1231.
14. Janbu, Nilmar, "Soil Compressibility as Determined by Oedometer and Triaxial Tests," European Conference on Soil Mechanics & Foundations Engineering, Wiesbaden, Germany Vol. 1, 1963, pp. 19–25.
15. Karst, H., et al. "Contribution à l'étude de la mecanique des milieux," *Proceedings of the 6th International Conference on Soil Mechanics and Foundations Engineering*, Vol. I, 1965, pp. 259–263.
16. Ko, H. Y., and Scott, R. F., "Deformation of Sand in Shear," *Journal of the Soil Mechanics and Foundations Division*, ASCE, Vol. 93, No. SM5, Proc. Paper 5470, September, 1967, pp. 283–310.
17. Kondner, R. L., "Hyperbolic Stress-Strain Response: Cohesive Soils," *Journal of the Soil Mechanics and Foundations Division*, ASCE, Vol. 89, No. SM1, Proc. Paper 3429, 1963, pp. 115–143.
18. Kondner, R. L., and Zelasko, J. S., "A Hyperbolic Stress-Strain Formulation for Sands," *Proceedings, 2nd Pan-American Conference on Soil Mechanics and Foundations Engineering*, Brazil, Vol. I, 1963, pp. 289–324.
19. Kondner, R. L., and Zelasko, J. S., "Void Ratio Effects on the Hyperbolic Stress-Strain Response of a Sand," Laboratory Shear Testing of Soils, ASTM *STP No. 361*, Ottawa, 1963.
20. Kondner, R. L., and Horner, J. M., "Triaxial Compression of a Cohesive Soil with Effective Octahedral Stress Control," *Canadian Geotechnical Journal*, Vol. 2, No. 1, 1965, pp. 40–52.
21. Kulhawy, F. H., and Duncan, J. M., "Finite Element Analysis of Stresses and Movements in Dams During Construction," *Report No. TE 69-4*, Office of Research Services, University of California, Berkeley, 1969.
22. Kulhawy, F. H., and Duncan, J. M., "Nonlinear Finite Element Analysis of Stresses and Movements in Oroville Dam," *Report No. TE 70-2*, Office of Research Services, University of California, Berkeley, 1970.
23. Lambe, T. W., "Methods of Estimating Settlement," *Journal of the Soil Mechanics and Foundations Division*, ASCE, Vol. 90, No. SM5, Proc. Paper 4060, September, 1964, pp. 43–67.
24. Lambe, T. W. "Stress Path Method," *Journal of the Soil Mechanics and Foundations Division*, ASCE, Vol. 93, No. SM6, Proc. Paper 5613, November, 1967, pp. 117–141.
25. Lee, Kenneth L., and Seed, H. Bolton, "Drained Strength Characteristics of Sands," *Journal of the Soil Mechanics and Foundations Division*, ASCE, Vol. 93, No. SM6, Proc. Paper 5561, November, 1967, pp. 117–141.
26. Makhlouf, H. M., and Stewart, J. J., "Factors Influencing the Modulus of Elasticity of Dry Sand," *Proceedings, 6th International Conference on Soil Mechanics and Foundations Engineering*, Montreal, Vol. 1, 1965, pp. 298–302.
27. Vesić, A. B., and Clough, G. W., "Behavior of Grandular Material under High Stresses," *Journal of the Soil Mechanics and Foundations Division*, ASCE, Vol. 94, No. SM3, Proc. Paper 5954, May, 1968, pp. 661–688.

APPENDIX II.—NOTATION

The following symbols are used in this paper: